Supporting Information

Reduced Graphene Oxide Induced Recrystallization of NiS Nanorods to Nanosheets and the Improved Na-Storage Properties

Qin Pan,[†,‡,] Jian Xie,[*,†,‡] Tiejun Zhu,[†] Gaoshao Cao,[‡] Xinbing Zhao,[*,†,‡] and Shichao Zhang[§]

[†] State Key Laboratory of Silicon Materials, Department of Materials Science and Engineering, Zhejiang University, Hangzhou 310027, China

[‡] Key Laboratory of Advanced Materials and Applications for Batteries of Zhejiang Province, China

[§] School of Materials Science and Engineering, Beijing University of Aeronautics and Astronautics, Beijing 100191, China

* Corresponding author. Tel./Fax: +86-571-87951451

E-mail: xiejian1977@zju.edu.cn, zhaoxb@zju.edu.cn

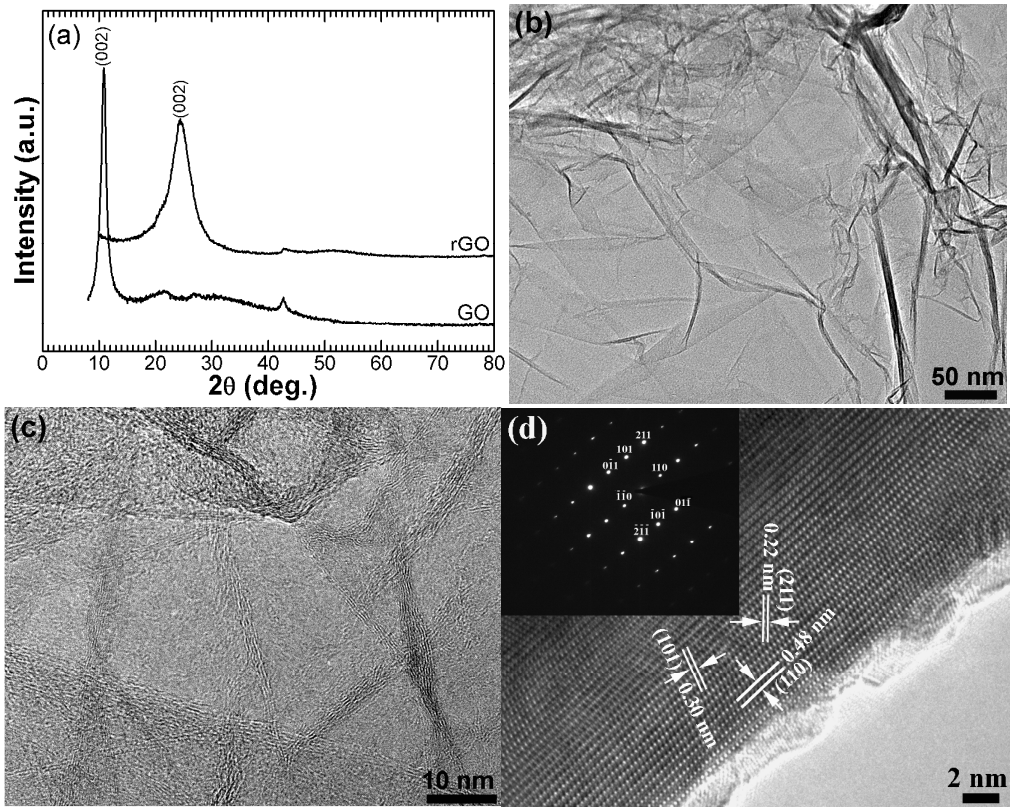

Figure S1. (a) XRD patterns GO and rGO, (b, c) TEM images of rGO, and (d) HRTEM image of an individual NiS nanorod.

In the above figure, it can be found that the characteristic peak (002 peak) of GO is positioned at around 10° (2θ) due to the presence of the oxygen-containing groups and the absorbed water.[1] The (002) peak of rGO shifts to around 25° (2θ), indicating the reduction of GO during the hydrothermal process.[2] The broad (002) diffraction peak of rGO compared with that of natural graphite is possibly due to the loss of long-range ordering.[3] TEM observation reveals the few-layer feature of rGO. Both GO and rGO were used to exfoliate NiS nanorod with an ex situ route by using pre-prepared NiS nanorods as the precursor in the hydrothermal reaction. HRTEM image and ED patterns indicate that the NiS nanorod shows a single-crystalline character.

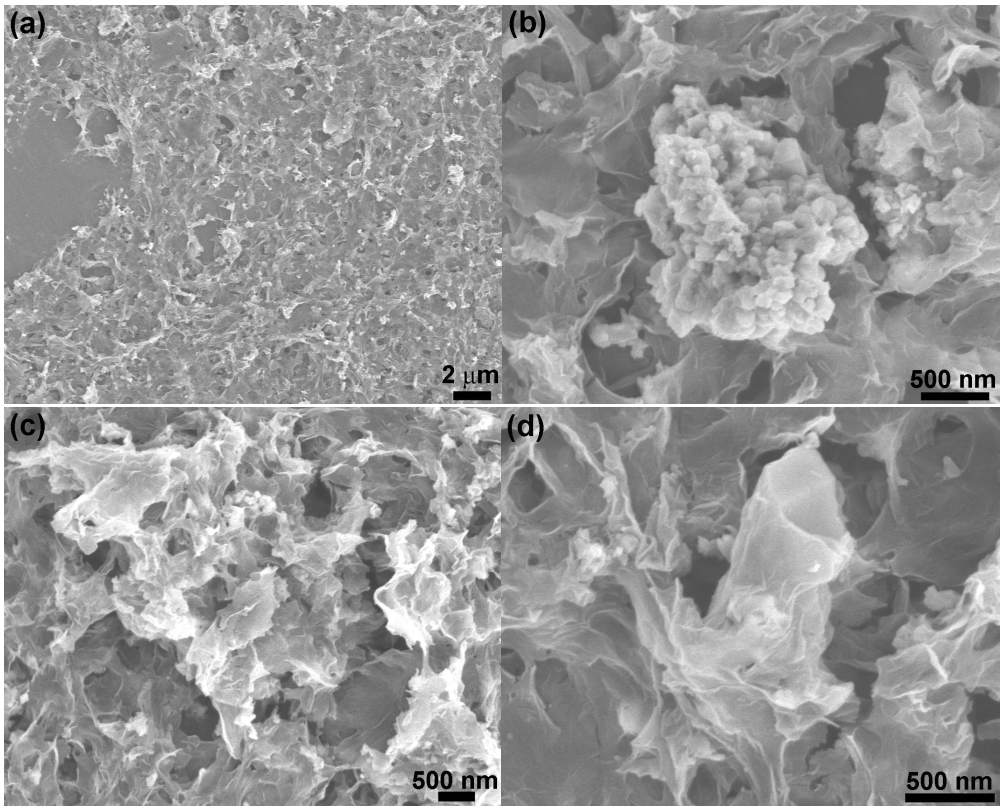

Figure S2. SEM images of NiS@20rGO-1 after the ex situ hydrothermal reaction.

The above figure shows some typical SEM images of the product after the ex situ hydrothermal reaction. The hydrothermal reaction was performed at 180 °C for 24 h using the pre-prepared NiS nanorods and rGO (Figure S1) as the precursors. The hydrothermal product is named NiS@20rGO-1. The images indicate that the original morphology of radially aggregated NiS nanorods disappears. Instead, typical structures of aggregated nanoparticles (Figure S2b), aggregated nanosheets (Figure S2c), or partially exfoliated individual nanorod (Figure S2d) can be seen. Clearly, these morphologies come from the exfoliation of NiS nanorods by rGO. The result implies that the NiS nanosheets originate from the exfoliation of NiS nanorods rather than from the direct nucleation/growth during the hydrothermal process.

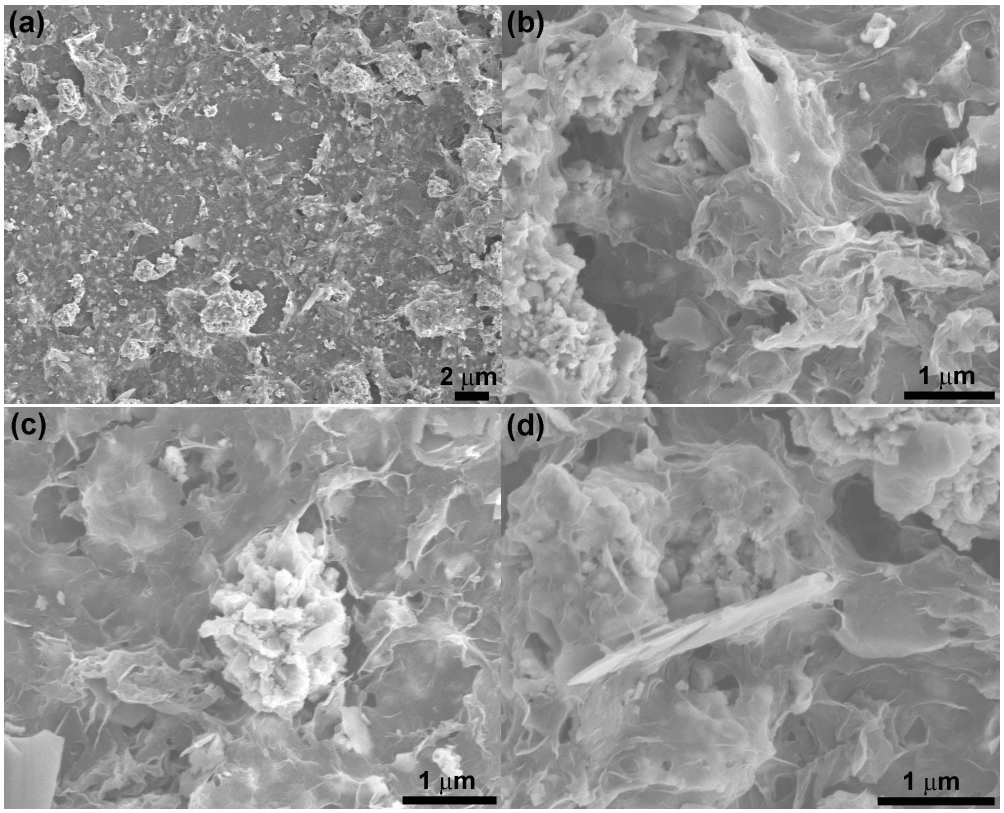

Figure S3. SEM images of NiS@20rGO-2 after the ex situ hydrothermal reaction.

The above figure exhibits some typical SEM images of the product after the ex situ hydrothermal reaction. The hydrothermal reaction was performed at 180 °C for 24 h using the pre-prepared NiS nanorods and GO as the precursors. The hydrothermal product is named NiS@20rGO-2. The images demonstrate that the original morphology of radially aggregated NiS nanorods also disappears. Instead, typical morphologies of aggregated nanosheets (Figure S3b), aggregated nanoparticles (or short nanorods, Figure S3c), or nearly completely exfoliated individual nanorod (Figure S3d) can be observed. Obviously, the recrystallization of NiS is related to the introduced GO. It is highly possible the actual component that exfoliates the NiS nanorods is rGO due to the fact that rGO itself can exfoliate NiS nanorods as discussed in Figure S2 and that GO can be reduced to rGO in a short time (Figure S5d). The result further confirms the assumption that the formation of NiS nanosheets is the result of the recrystallization of NiS nanorods.

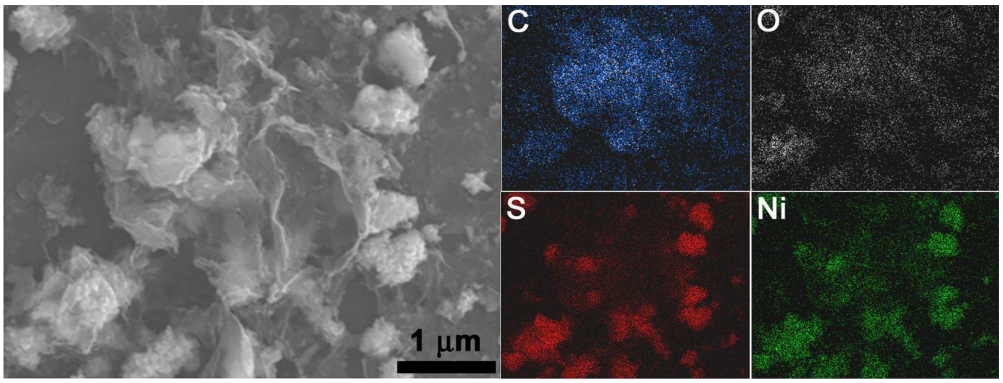

Figure S4. SEM image and EDS mapping of of NiS@20rGO-2 after the ex situ hydrothermal reaction.

From Figures S2 and S3, It can be seen that the recrystallization of NiS nanorods is not sufficient during the ex situ hydrothermal process. The aggregation of NiS nanosheets is evident by the EDS mapping as shown above. In addition, Carbon element mapping also indicates that the aggregation of rGO sheets also occurs due to the hydrophobic character of rGO. As a result, it is difficult to realize uniform dispersion of NiS nanosheets within rGO even using hydrophilic GO as the precursor. Therefore, an in situ hydrothermal route was used to prepare NiS/rGO composites with homogeneous dispersion of NiS sheets in rGO sheets. The in situ prepared products were systematically characterized to illuminate the exfoliation process and mechanism of NiS nanorods.

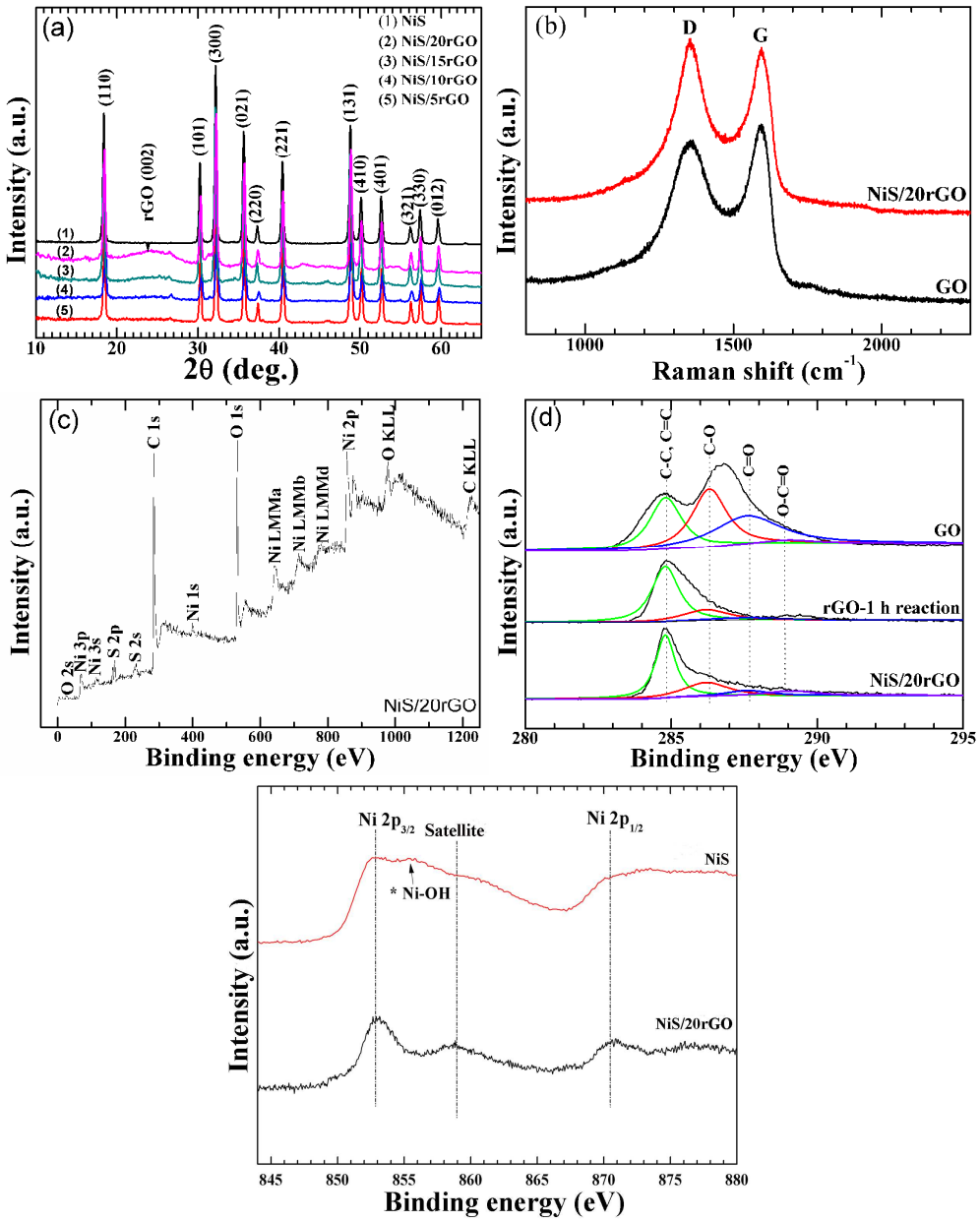

Figure S5. (a) XRD patterns of NiS and NiS/rGO composites, (b) Raman spectra of GO and NiS/20rGO, (c) XPS survey of NiS/20rGO, (d) C1s XPS of NiS/20rGO, GO, and rGO (hydrothermal reaction for 1 h), and (e) Ni2p XPS of NiS before and after the hydrothermal process.

The XRD patterns indicate that β-NiS forms (space group *R*3*m*, JCPDS No.03–0760) for bare NiS sample and all NiS/rGO samples and that (002) peak of rGO appears at high rGO content (Figure S5a). For Raman spectra, two peaks at 1350 and 1580 cm^{-1} are related to the disordered (D) band and graphitic (G) band of carbon-based materials (Figure S5b).[4] The rGO in NiS/20rGO exhibits an increased D/G intensity ratio than GO, indicating a decrease in the average size of sp^2 domains,[4] but an

increased number of sp^2 domains after reduction.[2] The XPS survey of NiS/20rGO shows the expected elements and their corresponding binding energy (Figure S5c). The C1s XPS in Figure S5d can be fitted into four peaks, corresponding to carbon atoms in different forms: non-oxygenated carbon (C–C, 285.6 eV, and C=C, 284.8 eV), carbon in C–O group (epoxy or hydroxyl, 286.3 eV), carbonyl carbon (C=O, 287.6 eV) and carboxyl carbon (O–C=O, 289.0 eV).[2,5] The remarkably decreased peak intensity of C–O, C=O and O–C=O groups suggests a sufficient reduction of GO after the hydrothermal reaction. Note that GO can be nearly reduced in a short time of 1 h. In Figure 5e, bare NiS nanorods show a broad peak at around 855 eV, which is related to the Ni-OH like species, in addition to the $Ni2p_{3/2}$, $Ni2p_{1/2}$ and the satellite peaks.[6] The Ni-OH like species may be on the surface of NiS nanorods, contributing to the exfoliation of NiS rods.

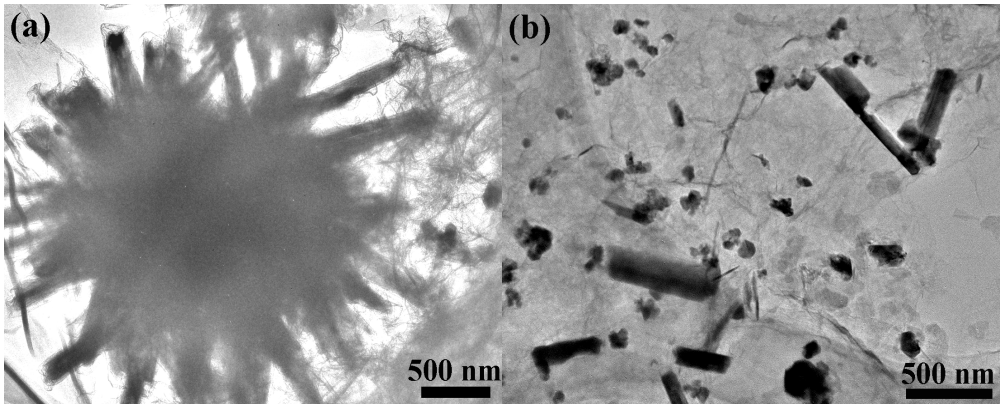

Figure S6. TEM images of (a) NiS/5rGO and (b) NiS/10rGO.

The above figure shows that at low rGO content, the aggregated rod-like structure of NiS, which is surrounded by rGO sheets, can be generally preserved (Figure S6a). However, the exfoliation of NiS nanorods does occur as evident from the presence of thin sheets around the rods and the "etching" of the ends of the rods. Increasing rGO content enhances the exfoliation of the nanorods (Figure S6b).

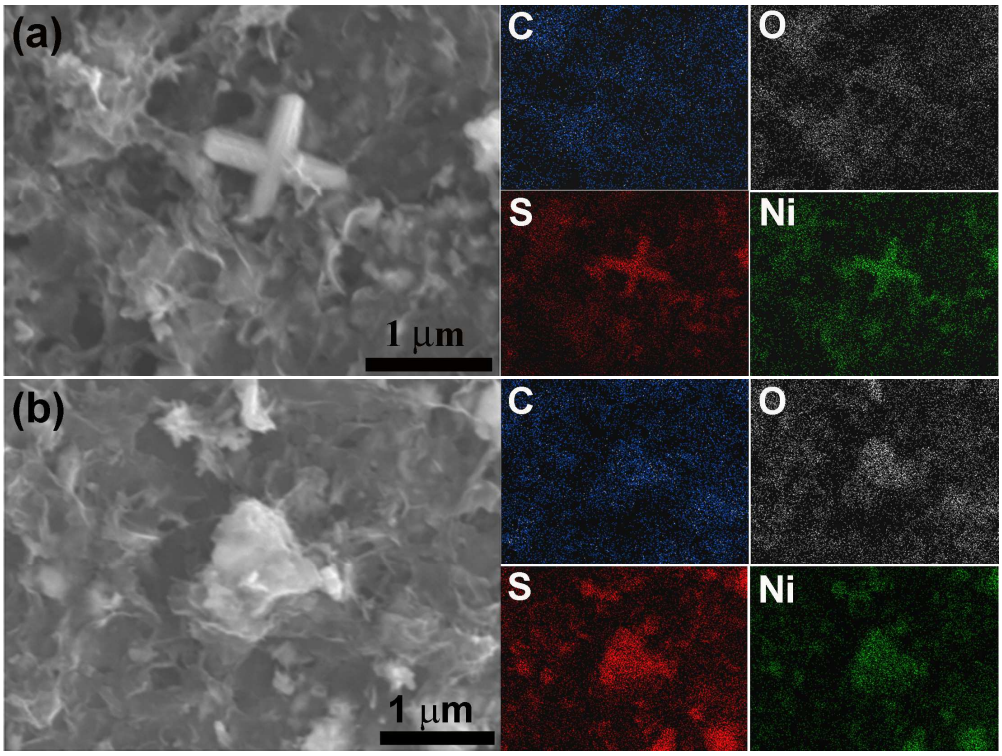

Figure S7. SEM images and EDS mapping of NiS/15rGO.

The EDS mapping confirms that the rod-like structure is the residual NiS nanorods and the aggregated sheet-like structure is the NiS nanosheets exfoliated from nanorods. Figures S7 indicates that even at 15 wt % rGO, it is difficult to obtain a complete exfoliation of NiS rods to sheets.

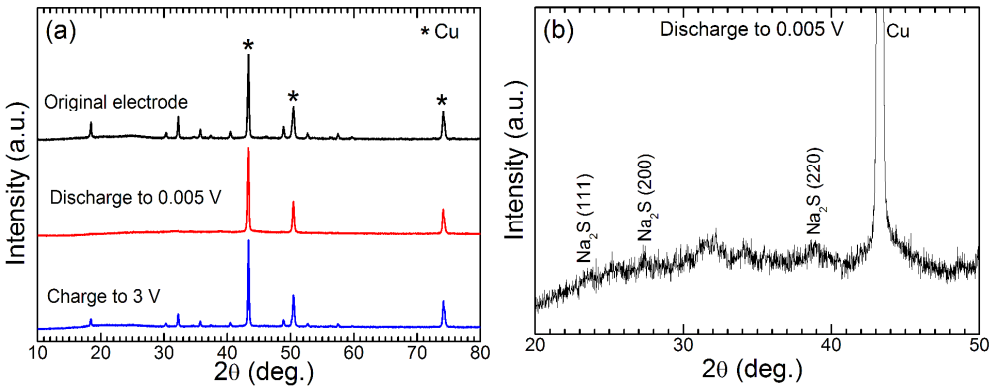

Figure S8. Ex situ XRD of NiS during discharge and charge.

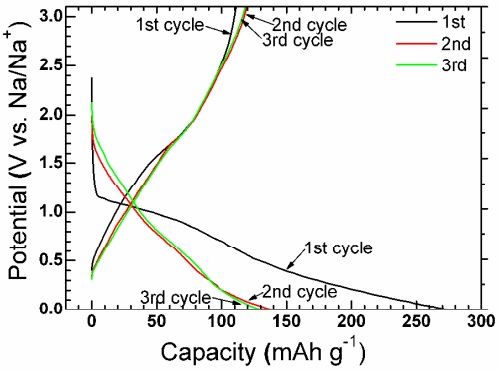

Figure S9. The first three charge and discharge curves of rGO at 50 mA g^{-1}.

REFERENCES

(1) Shi, H. J.; Kim, K. K.; Benayad, A.; Yoon, S. M.; Park, H. K.; Jung, I. S.; Jin, M. H.; Jeong, H. K.; Kim, J. M.; Choi, J. Y.; Lee, Y. H. *Adv. Funct. Mater.* **2009**, *19*, 1987–1992.

(2) Stankovich, S.; Dikin, D. A.; Piner, R. D.; Kohlhaas, K. A.; Kleinhammes, A.; Jia, Y. Y.; Wu, Y.; Nguyen, S. T.; Ruoff, R. S. *Carbon* **2007**, *45*, 1558–1565.

(3) McAllister, M. J.; Li, J. L.; Adamson, D. H.; Schniepp, H. C.; Abdala, A. A.; Liu, J.; Herrera Alonso, M.; Milius, D. L.; Car, R.; Prud'homme, R. K.; Aksay, I. A. *Chem. Mater.* **2007**, *19*, 4396–4404.

(4) Tuinstra, F.; Koenig, J. L. *J. Chem. Phys.* **1970**, *53*, 1126–1130.

(5) Dubin, S.; Gilje, S.; Wang, K.; Tung, V. C.; Cha, K.; Hall, A. S.; Farrar, J.; Varshneya, R.; Yang, Y.; Kaner, R. B. *ACS Nano* **2010**, *4*, 3845–3852.

(6) Legrand, D. L.; Nesbitt, H. W.; Bancroft, G. M. *Am. Mineral.* **1998**, *83*, 1256–1265.